

Charge excitations associated with charge stripe order in the 214-type nickelate and superconducting cuprate

S. Wakimoto,¹ H. Kimura,² K. Ishii,³ K. Ikeuchi,³ T. Adachi,⁴ M. Fujita,⁵ K. Kakurai,¹
Y. Koike,⁴ J. Mizuki,³ Y. Noda,² A. H. Said,⁶ Y. Shvyd'ko,^{6,7} and K. Yamada^{5,7}

¹ Quantum Beam Science Directorate, Japan Atomic Energy Agency, Tokai, Ibaraki 319-1195, Japan

² Institute of Multidisciplinary Research for Advanced Materials, Tohoku University, Sendai 980-8577, Japan

³ Synchrotron Radiation Research Unit, Japan Atomic Energy Agency, Hyogo 679-5148, Japan

⁴ Department of Applied Physics, Tohoku University, Sendai 980-8579, Japan

⁵ Institute for Materials Research, Tohoku University, Katahira, Sendai 980-8577, Japan

⁶ Advanced Photon Source, Argonne National Laboratory, Argonne, Illinois 60439, USA

⁷ Advanced Institute for Materials Research, Katahira, Sendai 980-8577, Japan

(Dated: February 2, 2022)

Charge excitations were studied for stripe-ordered 214 compounds, $\text{La}_{5/3}\text{Sr}_{1/3}\text{NiO}_4$ and 1/8-doped $\text{La}_2(\text{Ba}, \text{Sr})_x\text{CuO}_4$ using resonant inelastic x-ray scattering in hard x-ray regime. We have observed charge excitations at the energy transfer of ~ 1 eV with the momentum transfer corresponding to the charge stripe spatial period both for the diagonal (nickelate) and parallel (cuprates) stripes. These new excitations can be interpreted as a collective stripe excitation or charge excitonic mode to a stripe-related in-gap state.

There is accumulation of theoretical and experimental implications that the inhomogeneous charge state, such as a charge stripe state, occurring as a result of the carrier doping into the strongly correlated electron system is intimately related to the realization of high temperature superconductivity in cuprates [1, 2]. Understanding the dynamics of the charge stripe state is one of the basic problems. To date, whereas the dynamics in spin sector has been studied extensively by neutron scattering [3, 4, 5, 6], the dynamics in charge sector is yet to be understood.

The 214 type nickelates and cuprates, family compounds of the firstly discovered high temperature superconductor $\text{La}_{2-x}\text{Ba}_x\text{CuO}_4$, exhibit charge stripe order when holes are doped. The stripe order has been comprehensively studied by diffraction techniques [7, 8, 9, 10] and characterized by antiphase antiferromagnetic domains divided by one dimensional charge stripes where doped holes are confined. Upon carrier doping, $\text{La}_{2-x}\text{Sr}_x\text{NiO}_4$ (LSNO) shows ordered state of “diagonal” stripes, where the charge stripes run along the diagonal direction of the NiO_2 square lattice [7] (Fig. 1 a). Hole-doped 214 cuprates $\text{La}_{2-x}(\text{Ba}, \text{or Sr})_x\text{CuO}_4$ (LBCO or LSCO) show diagonal stripe order in the low doping insulating region [11], whereas in the superconducting dome the systems, particularly LBCO, show static order of “parallel” stripes only in the vicinity of $x = 0.125$ [12, 13] where the superconductivity is suppressed [14]. This is frequently quoted as 1/8 anomaly. Here the charge stripes are parallel to the Cu-O-Cu bond (Fig. 1 b). Consequently, relation between the dynamical fluctuation of parallel stripes and the superconductivity is of interest.

Resonant inelastic x-ray scattering (RIXS) in hard x-ray regime, a recently developed experimental probe, have revealed various types of charge excitations in the strongly correlated electron systems, such as the charge

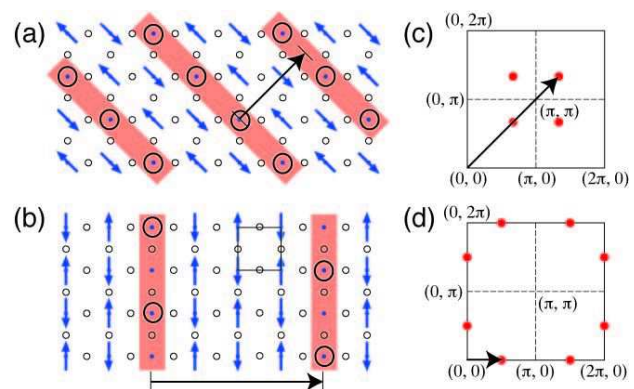


FIG. 1: (Color online) Diagonal charge stripes in (a) LSNO $x = 1/3$ and parallel stripes in (b) LBCO $x = 0.125$ and LSCO $x = 0.12$ in the basal (Ni, or Cu) O_2 plane. Stripes are marked by shaded belts. (c) and (d) depict momentum space for the (Ni or Cu) O_2 square lattice in unit of $1/a$ (a is the lattice constant of the square lattice). Arrows connecting the stripes in (a) and (b) indicate spatial periods of stripes. Arrows in (c) and (d) indicate characteristic momentum transfer \mathbf{q}_s . The period of $(3a/2, 3a/2)$ in (a) gives characteristic momentum transfer $\mathbf{q}_s = (2\pi/3, 2\pi/3)$, and the period of $(4a, 0)$ in (b) gives $\mathbf{q}_s = (\pi/2, 0)$. Circles in (c) and (d) indicate equivalent \mathbf{q}_s points due to the stripe domains whose stripes run perpendicular with each other.

excitation across the charge transfer (CT) gap [15, 16, 17, 18], intraband excitations [18], molecular orbital excitations [19], $d-d$ excitations [17], collective charge excitations [20], and even magnons [21]. The major advantage of RIXS is the possibility of studying charge excitations as a function of the momentum transfer \mathbf{q} . The stripe spacing in the real space corresponds to a characteristic momentum transfer \mathbf{q}_s as shown in Figs. 1 c and 1 d. RIXS is an ideal probe for detecting charge excitations associated with the stripe having a specific momentum

transfer \mathbf{q}_s .

In this Letter, we report the first observation of charge excitations arising from the charge stripe ordered state in 214 type nickelate, $\text{La}_{5/3}\text{Sr}_{1/3}\text{NiO}_4$, and 214 type superconducting cuprates $\text{La}_{1.875}\text{Ba}_{0.125}\text{CuO}_4$ and $\text{La}_{1.88}\text{Sr}_{0.12}\text{CuO}_4$ using the RIXS in hard x-ray regime. Our measurements reveal the charge excitations with the momentum transfer corresponding to the charge stripe spatial period. We observe this nontrivial feature both for the diagonal (nickelate) and parallel (cuprates) stripes.

Single crystals of LSNO $x = 1/3$, LBCO $x = 0.125$, LBCO $x = 0.08$, and LSCO $x = 0.12$ were prepared by the travelling solvent floating zone method. The samples of LSNO $x = 1/3$ and LBCO $x = 0.125$ show robust charge stripe order below 180 K and 55 K, respectively. LBCO $x = 0.08$ shows no clear stripe order according to the neutron diffraction studies. LSCO $x = 0.12$ is expected to have stripe order below 30 K from neutron diffraction, but charge order has not been confirmed directly. Lattice constants for LSNO and L(B,S)CO at low temperatures give reciprocal lattice unit of 1.66 \AA^{-1} for the basal (Ni, or Cu) O_2 square lattices. The RIXS measurements of nickelate were performed at 10 K using the MERIX spectrometer installed at the Advanced Photon Source, beamline XOR-IXS 30-ID. RIXS measurements of cuprates were done at 8 K using the inelastic x-ray spectrometer at BL11XU at SPring-8. Horizontal scattering geometry was utilized for all measurements, with the scattering plane parallel to the (a, c) crystal plane. Since the 214 compounds are two dimensional, we assign the $(0, 0, L)$ position as the Γ point $(0, 0)$ of the basal plane and $(1, 0, L)$ as the next Γ point $(2\pi, 0)$. Here L is chosen so that the scattering angle 2θ is $\sim 90^\circ$. In this configuration the scattered photon propagates parallel to the polarization of the initial photon, and thus, minimizes the elastic intensity. This is crucial for observing the low energy excitations below 1.5 eV reported in this Letter.

RIXS in the hard x-ray regime uses incident photons with the energy at the absorption K-edge of the transition metal element. Incident photons excite $1s$ core electrons into either $4p_\pi$ or $4p_\sigma$ orbitals depending on the sample geometry, and this intermediate state triggers various charge excitations. In the present studies the incident photon energy was tuned to the energy of the $1s \rightarrow 4p_\pi$ transition, which is 8347 eV for nickelate and 8993 eV for cuprates. These energies are a few electron volts lower than the energy of the $1s \rightarrow 4p_\sigma$ transition. The instrumental energy resolution of the MERIX spectrometer at Ni K-edge is 150 meV. This is achieved by using a Ge(642) spherical diced analyzer, and a position sensitive microstrip detector placed on the Rowland circle of a 1 m radius. The silicon microstrip detector with $125 \mu\text{m}$ pitch is applied with the purpose of reducing the geometrical broadening of the spectral resolution function [22]. The energy resolution of the Cu K-edge RIXS

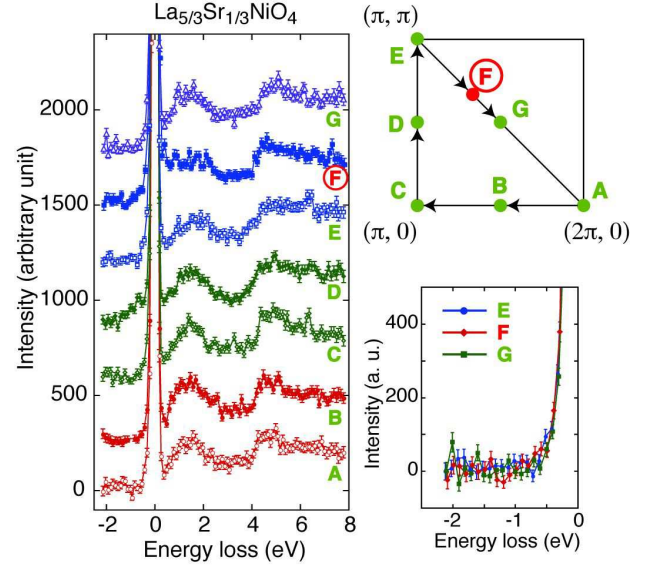


FIG. 2: (Color online) RIXS spectra for LSNO $x = 1/3$ at several \mathbf{q} positions. Each spectrum is shifted by 300 in intensity for clarity. Measured \mathbf{q} positions are indicated in the right top figure by circles labeled as A to G connected by allows, where the allows show the order of spectra from the bottom to the top. The point, labeled F, is \mathbf{q}_s . The right bottom figure shows comparison of elastic tails on the energy gain side of the RIXS spectra for positions at E, F, and G.

spectrometer at BL11XU is 400 meV. Bent Ge(337) analyzer with 2 m curvature radius and a point silicon detector is used. q -resolutions of MERIX with the present configuration are 0.26 \AA^{-1} and 0.38 \AA^{-1} along the $[\pi, 0]$ and $[0, \pi]$ directions, respectively. Those for BL11XU are 0.10 \AA^{-1} and 0.15 \AA^{-1} , respectively.

Figure 2 shows representative RIXS spectra for LSNO $x = 1/3$ taken at the \mathbf{q} positions indicated in the right top panel. Every spectrum except that at $\mathbf{q}_s = (4\pi/3, 2\pi/3)$ (labeled as F), contains mainly three peaks: an elastic peak at zero energy, and peaks at $\sim 1.5 \text{ eV}$ and $\sim 4.5 \text{ eV}$. The 4.5 eV feature is known to be the charge excitation across the CT gap (called a CT peak), which is also observed in the non-doped La_2NiO_4 [17]. The 1.5 eV feature can be attributed to the charge excitation from the valence band to the in-gap band which is known to appear when holes are doped into nickelates by optical measurements [24, 25, 26]. There is a dip between the elastic peak and the in-gap peak implying a gap in charge excitation, consistent with the fact that the nickelate is an insulator. However, to our surprise, the dip appears to be filled at $\mathbf{q} = \mathbf{q}_s$. We note that the elastic peak at $\mathbf{q} = \mathbf{q}_s$ is twice as strong as those at the other \mathbf{q} positions due to the charge stripe order [23]. One might suspect that the additional intensity comes from the tail of the stronger elastic peak. However, as clearly seen in the right bottom panel of Fig. 2, the intensity of the elastic peak tail on the energy gain side at $\mathbf{q} = \mathbf{q}_s$ is same as for

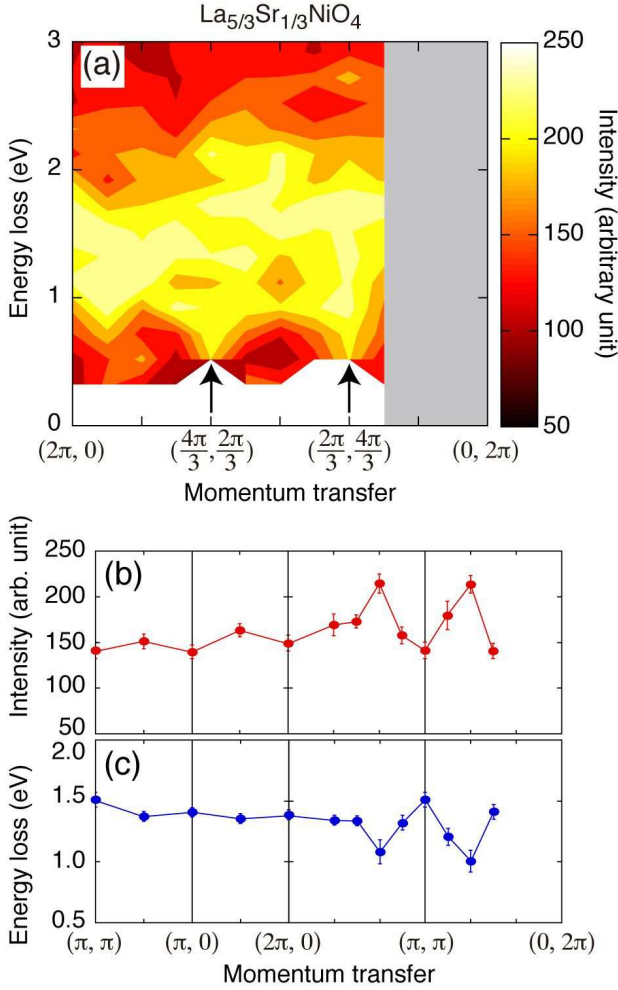


FIG. 3: (Color online) (a) A contour plot of the RIXS intensity between $(2\pi, 0)$ and $(0, 2\pi)$. The white area has intensity more than 250 due to elastic peak or filled dip at \mathbf{q}_s positions. The shaded rectangular area has not been measured. (b) \mathbf{q} dependence of the RIXS intensity averaged in the energy region between 0.5 and 0.9 eV (upper panel) and the position of the in-gap peak (lower panel).

other \mathbf{q} positions. This rules out such explanation.

We have measured RIXS spectra at several \mathbf{q} -positions between $(2\pi, 0)$ and $(0, 2\pi)$ to test if the filled gap is unique at \mathbf{q}_s . The RIXS intensities are mapped in Fig. 3 a as a contour plot. It is clearly demonstrated that the dip between the elastic and the in-gap peaks is indeed absent at both \mathbf{q}_s positions, $(4\pi/3, 2\pi/3)$ and $(2\pi/3, 4\pi/3)$. Correspondingly, the RIXS signal averaged in the energy region between 0.5 and 0.9 eV has maxima at \mathbf{q}_s (Fig. 3 b). Figure 3 c shows in-gap peak positions obtained by fitting the RIXS spectra above 0.4 eV to a function with two Lorentzians and sloped background. It is shown that the in-gap feature is primarily independent of \mathbf{q} but the anomaly appears at \mathbf{q}_s due to the filled dip.

As a next step we will compare the LSNO results with those of cuprates whose representative RIXS spectrum is

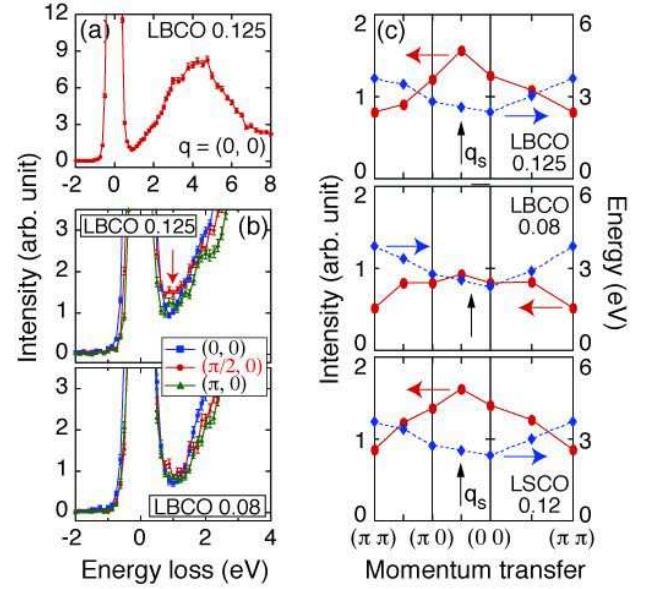


FIG. 4: (Color online) (a) Representative RIXS spectrum of LBCO $x = 0.125$ at zone center. (b) Close-ups of RIXS spectra around 1 eV of LBCO $x = 0.125$ (upper) and LBCO $x = 0.08$ (lower) measured at $(0, 0)$, $(\pi/2, 0)$, and $(\pi, 0)$. RIXS intensities are normalized to the maximum of the CT peak at ~ 4 eV. The arrow in (b) highlights anomalous enhancement of RIXS intensity around 1 eV at $\mathbf{q}_s = (\pi/2, 0)$ observed in LBCO $x = 0.125$. (c) Momentum transfer dependence of the RIXS signal averaged in the energy region between 1 and 1.25 eV (circles) and the energy where the RIXS intensity reaches the half-maximum of the CT peak (diamonds). Arrows in (c) indicate \mathbf{q}_s positions. Although the LBCO $x = 0.08$ sample does not have robust stripe order, it may have very small signal of static order with $\mathbf{q}_s = 2\pi(2x, 0)$ as observed in underdoped LSCO [31]. The arrow in the middle panel of (c) indicates this $\mathbf{q}_s = (0.32\pi, 0)$ for LBCO $x = 0.08$ as a reference.

shown in Fig. 4 a. All spectra we observed contain two peaks; the elastic peak and the CT peak at ~ 4 eV. In the case of cuprates, the in-gap peaks are not observed clearly. It was earlier reported that the continuum-like intensity near 1 eV increases with doping [27] due to the increase of free (conductive) holes [28]. A similar effect is seen in Fig. 4 b, showing the spectra of LBCO $x = 0.125$ and 0.08. The parallel stripe order with a $4a$ spacing, which realizes in LBCO $x = 0.125$ and LSCO $x = 0.12$, gives \mathbf{q}_s at $(\pi/2, 0)$ (Fig. 1 c). Remarkably, we have found an anomalous enhancement of the RIXS intensity near 1 eV at $\mathbf{q}_s = (\pi/2, 0)$ in the stripe ordered samples. This is more clearly demonstrated in Fig. 4 c, where the RIXS intensity averaged in the energy range between 1 and 1.25 eV (circles) peaks at \mathbf{q}_s in LBCO $x = 0.125$ and LSCO $x = 0.12$. On the contrary, it is flat in the non-stripe ordered LBCO $x = 0.08$. Diamonds in Fig. 4 c indicate the energy position where the CT peak reaches a half of its maximal intensity. This quantity increases, that is, the CT peak shifts to the higher en-

ergy, as \mathbf{q} changes from $(0, 0)$ to $(\pi, 0)$ for all compounds. Upon the same change of \mathbf{q} , the elastic peak intensity decreases [23]. These facts evidence that the enhancement of the RIXS intensity at ~ 1 eV relates to an intrinsic property of the system, and cannot be explained by the overlap of the tails of the elastic and CT peaks.

The above presented data on nickelate and cuprates demonstrate that the charge stripe state gives the additional RIXS intensity near 1 eV at the \mathbf{q}_s positions regardless of the stripe geometry. Here we discuss possible origins of the discovered excitation. The calculations presented in Ref. [29] predicted that the parallel stripes are accompanied by collective charge excitations with the momentum transfer \mathbf{q}_s . Qualitatively similar excitations are expected for the diagonal stripes. RIXS can detect such excitations. Therefore, it is reasonable to attribute the observed additional intensity at $\mathbf{q} = \mathbf{q}_s$ in the RIXS spectra of Figs. 2 and 4 to the collective stripe excitations. The instrumental resolutions in energy and momentum transfer of current setups are not good enough to see detailed structure of dispersion. Nevertheless the presented results demonstrate the potential of the RIXS technique for observing collective charge stripe excitations.

Another plausible explanation is that the anomaly at \mathbf{q}_s is the nature of charge exciton to the in-gap state; that is, the excitonic mode has anomalous softening at \mathbf{q}_s . An exciton is the bound state between an excited electron to the in-gap band and a left hole in the valence band, and hence the exciton spectrum must be always gapped. In this case, the anomalous softening of the exciton mode gives smaller gap at \mathbf{q}_s which we estimate to be less than 340 meV for nickelate and less than 800 meV for cuprates from the instrumental resolution.

It is not an easy task to distinguish between the above two possibilities. The collective charge excitation should be possible to be detected by non-resonant IXS whereas a creation of the charge exciton requires the resonant process. Thus performing the non-resonant IXS is one way to proceed. However, intensity of the collective charge excitation might be extremely small. Also, theoretical calculations of in-gap band are desirable to examine the excitonic possibility. The origin of the in-gap state has been interpreted in many ways [25, 26, 30]. The present observation evidences the connection between the in-gap state and the stripe. It is important to test if the softening of excitonic mode is reproducible by taking the charge stripe structure into account whatever the origin of the in-gap state is.

In summary, we have performed RIXS measurements in hard x-ray regime of the stripe-ordered 214 type nickelate and superconducting cuprates. We have observed for the first time charge excitations at the characteristic momentum transfer \mathbf{q}_s related to the spatial period of the stripes. They can be interpreted as a collective stripe excitation or charge excitonic mode to a stripe-related

in-gap state.

Authors thank E. Kaneshita, K. Machida, and K. Nakajima for invaluable discussions, and Peter Siddons (BNL) for building the microstrip detector of MERIX. This work is partially supported by a Grant-In-Aid from the Japanese Ministry of Education, Culture, Sports, Science and Technology. Use of the Advanced Photon Source was supported by the U. S. Department of Energy, Office of Science, Office of Basic Energy Sciences, under Contract No. DE-AC02-06CH11357.

-
- [1] S. A. Kivelson, *et al.*, Rev. Mod. Phys. **75**, 1201 (2003).
 - [2] J. Zaanen, O. Y. Osman, H. V. Kruis, Z. Nussinov, and J. Tworzydło, Phil. Mag. B **81**, 1485 (2001).
 - [3] R. J. Birgeneau, C. Stock, J. M. Tranquada, and K. Yamada, J. Phys. Soc. Jpn. **75**, 111003 (2006).
 - [4] S. M. Hayden, H. A. Mook, P. Dai, T. G. Perring, and F. Doğan, Nature **429**, 531 (2004).
 - [5] J. M. Tranquada *et al.*, Nature **429**, 534 (2004).
 - [6] H. Woo *et al.*, Phys. Rev. B **72**, 064437 (2005).
 - [7] J. M. Tranquada, D. J. Buttrey, and V. Sachan, Phys. Rev. B **54**, 12318 (1996).
 - [8] A. Vigliante *et al.*, Phys. Rev. B **56**, 8248 (1997).
 - [9] J. M. Tranquada, B. J. Sternlieb, J. D. Axe, Y. Nakamura, and S. Uchida, Nature **375**, 561 (1995).
 - [10] M. v. Zimmermann *et al.*, Europhysics Letters **41**, 629 (1998).
 - [11] S. Wakimoto *et al.*, Phys. Rev. B **60**, R769 (1999).
 - [12] T. Suzuki *et al.*, Phys. Rev. B **57**, R3229 (1998).
 - [13] M. Fujita, H. Goka, K. Yamada, J. M. Tranquada, and L. P. Regnault, Phys. Rev. B **70**, 104517 (2004).
 - [14] A. R. Moodenbaugh, Youwen Xu, M. Suenaga, T. J. Folkerts, and R. N. Shelton Phys. Rev. B **38**, 4596 (1988).
 - [15] M. Z. Hasan *et al.*, Science **288**, 1811 (2000).
 - [16] Y.-J. Kim *et al.*, Phys. Rev. Lett. **89**, 177003 (2002).
 - [17] E. Collart *et al.*, Phys. Rev. Lett. **96**, 157004 (2006).
 - [18] K. Ishii *et al.*, Phys. Rev. Lett. **94**, 207003 (2005).
 - [19] Y.-J. Kim *et al.*, Phys. Rev. B **70**, 205128 (2004).
 - [20] L. Wray *et al.*, Phys. Rev. B **76**, 100507(R) (2007).
 - [21] J. P. Hill *et al.*, Phys. Rev. Lett. **100**, 097001 (2008).
 - [22] S. Huotari *et al.*, J. of Synchrotron Radiation **12**, 467 (2005).
 - [23] For the nickelate, L of the \mathbf{q} was chosen at each \mathbf{q} to satisfy $2\theta = 90^\circ$, while for cuprates L was fixed at 13.5. The enhancement of the elastic peak at \mathbf{q}_s in nickelate is mainly due to the additional elastic scattering from the charge order. The decrease of the elastic intensity in cuprates by moving from $(0,0)$ to $(\pi,0)$ is due to the decreasing elastic scattering while approaching $2\theta = 90^\circ$.
 - [24] T. Ido, K. Magoshi, H. Eisaki, and S. Uchida, Phys. Rev. B **44**, 12094 (1991).
 - [25] T. Katsufuji *et al.*, Phys. Rev. B **54**, R14230 (1996).
 - [26] C. C. Homes, J. M. Tranquada, Q. Li, A. R. Moodenbaugh, D. J. Buttrey, Phys. Rev. B **67**, 184516 (2003).
 - [27] Y.-J. Kim *et al.*, Phys. Rev. B **70**, 094524 (2004).
 - [28] S. Uchida *et al.*, Phys. Rev. B **43**, 7942 (1991).
 - [29] E. Kaneshita, M. Ichioka, and K. Machida, Phys. Rev. Lett. **88**, 115501 (2002).
 - [30] K. Tsutsui, W. Koshibae, and S. Maekawa, Phys. Rev.

B **59**, 9729 (1999).

[31] H. Hiraka *et al.*, J. Phys. Soc. Jpn. **70**, 853 (2001).